International Journal of Pharmaceutics 585 (2020) 119474

Contents lists available at ScienceDirect

International Journal of Pharmaceutics

journal homepage: www.elsevier.com/locate/ijpharm

Bioresponsive nanostructured systems for sustained naltrexone release and treatment of alcohol use disorder: Development and biological evaluation

Rogério A. Santos, Mariana Rae, Vanessa F.M.C. Dartora, Jenyffer K.R. Matos, Rosana Camarini, Luciana B. Lopes*

Department of Pharmacology, Instituto de Ciências Biomédicas – Universidade de Sao Paulo, Brazil

ARTICLE INFO

Keywords:
Microemulsion
In vivo swelling
Hexagonal phase
Sustained release
Naltrexone
Alcohol use disorder

ABSTRACT

In this study, microemulsions capable of transforming into nanostructured hexagonal phase gels *in vivo* upon uptake of biological fluids for naltrexone prolonged release were investigated as a strategy for management of alcohol use disorder (AUD). Microemulsions were prepared using monoolein, tricaprylin, water and propylene glycol; after preliminary characterization, one formulation was selected, which contained 55% of monoolein-tricaprylin (M − 55). This microemulsion displayed size below 200 nm and Newtonian rheological behavior. Liquid crystalline gels formed *in vitro* upon 8 h of contact with water following a second order kinetics. After 120 h, < 50% of naltrexone was released *in vitro* independently on drug loading (5 or 10%). *In vivo,* gels formed within 24 h of M − 55 subcutaneous administration, and persisted locally for over 30 days providing slow release of the fluorescent marker Alexa fluor compared to a solution. Using the conditioned place preference paradigm, a test used to measure drug's rewarding effects, a single dose of M − 55 containing 5% naltrexone reduced the time spent in the ethanol-paired compartment by 1.8-fold compared to saline; this effect was similar to that obtained with daily naltrexone injections, demonstrating the formulation efficacy and its ability to reduce dosing frequency. A more robust effect was observed following administration of M − 55 containing 10% of naltrexone, which was compatible with aversion. These results support M − 55 as a platform for sustained release of drugs that can be further explored for management of AUD to reduce dosing frequency and aid treatment adherence.

1. Introduction

Substance use disorders is a worldwide problem associated with serious health, social, and economic burden, often resulting in lower life expectancy compared to the general population (Carvalho et al., 2019a; Manthey et al., 2019; Patel et al., 2016). Among the many forms of substance use disorders, those related to alcohol use are among the most common, and present relatively few treatment options (Manthey et al., 2019). Oral administration of naltrexone, an opioid antagonist, is used in detoxified patients to prevent relapses. In addition, naltrexone has been employed and/or studied for treatment and prevention of relapse in opioid, methamphetamine, gambling and cocaine (the later in association with other compounds) addiction (Boudreau et al., 2020; Guo et al., 2019; Sushchyk et al., 2016; Victorri-Vigneau et al., 2018).

Oral dosing regimens ranging from 50 to 100 mg of naltrexone daily to three times/week have been used for treatment of alcohol use disorder (Lobmaier et al., 2010; Schmitz et al., 2009), but efficacy is limited by the extensive first-pass hepatic metabolism of the drug, which results in low bioavailability (5–40%) (Lobmaier et al., 2010; Yin et al., 2002). Efficacy is further complicated by the high frequency of administration required, which together with the lack of pleasurable feelings following naltrexone intake, reduces patient compliance. To overcome these problems, incorporation of naltrexone in delivery systems that can be administered through alternative routes and provide prolonged release (keeping effective and relatively constant plasma levels) have attracted interest.

A wide variety of innovative systems capable of providing sustained or controlled release of drugs has been studied, such as hydrogel-forming microneedles, electrospun nanofiber materials, tablets with bespoken geometry, buccal polymeric bioadhesive wafers and tablets, and thermoresponsive poly (N-isopropylacrylamide) particles (Chen et al., 2020; Courtenay et al., 2020; Giannola et al., 2007; Giordani et al., 2020; Kyobula et al., 2017; McMasters et al., 2017; Yang et al., 2019). Delivery systems investigated to prolong naltrexone release include intramuscular polymeric microparticles, transdermal devices, buccal tablets and subcutaneous gels and implants (Giannola et al., 2007; Johnson, 2007; Milewski and Stinchcomb, 2011; Ngo et al., 2008; Yin et al., 2002). Among them, microparticles for intramuscular

* Corresponding author at: Instituto de Ciências Biomédicas, Universidade de Sao Paulo, Av. Prof. Lineu Prestes 1524, São Paulo - SP, Brazil.
E-mail address: lublopes@usp.br (L.B. Lopes).

https://doi.org/10.1016/j.ijpharm.2020.119474
Received 4 March 2020; Received in revised form 22 May 2020; Accepted 24 May 2020
Available online 27 May 2020
0378-5173/

injection and subcutaneous polymeric implants have been approved or are under clinical trials for alcohol and/or opioid addiction. In spite of their benefits, both dosage forms have drawbacks: production of microparticles and implants is a multi-step and expensive process, their administration requires trained personnel and health care settings, and implants require surgical procedures to insert, and very often, remove them (Hulse et al., 2005; Johnson, 2007). Additionally, implants have a higher risk of local reactions (due to their longer residence time), and unsafe overdosage in case of manufacture-related problems, leading to drug release over too short a time interval (Collet and Moreton, 2007; Hulse et al., 2005; Kurnatowska et al.; Roozen et al., 2007). Therefore, simple formulations that can be easily obtained and administered, causing minimal local reactions are still needed. To fill this gap, this study aimed at developing and assessing the *in vivo* efficacy of bioresponsive microemulsions for subcutaneous injection and spontaneous transformation into reverse hexagonal phase gels upon absorption of interstitial water.

The hexagonal phase has been described as cylinders of micelles arranged as a hexagon, and demonstrated to prolong the release of hydrophilic and lipophilic compounds (Drummond and Fong, 2000; Muller-Goymann, 2004). Two types have been described: the reverse type, in which water and hydrophilic drugs are enclosed within the cylinders, and the normal type, in which water is found outside of the cylinders (Borne et al., 2003; Rizwan et al., 2009; Wang et al., 2006). We have previously studied BRIJ (polyoxyethylene 10 oleoyl ether)-based normal type hexagonal phases as naltrexone delivery system, but because this system dissolved in contact with aqueous fluids within 96 h, we anticipated that frequent administration would be required. To overcome this problem, microemulsions composed of the polar lipid monoolein, capable of *in situ* transformation into reverse hexagonal phases and of resisting dilution for longer periods (Boyd et al., 2006; Depieri et al., 2016; Fong et al., 2009) were investigated in the present study.

Compared to other naltrexone prolonged release systems, the formulation proposed here offers several advantages, including: (i) the precursor microemulsion is easy to prepare and thermodynamically stable, enabling reduction of costs and long shelf-life; (ii) the subcutaneous route is considered to be superior to other routes in terms of naltrexone potency, and administration through this route does not require extensive personnel training, enabling family members to perform it (similarly to insulin); and (iii) the administration site of subcutaneous injections can be alternated to reduce local reactions (Al-Tahami et al., 2011; Fong et al., 2009; Hosmer et al., 2011; Ruel-Gariepy and Leroux, 2004; Williams and Broadbridge, 2009).

In this study, microemulsions composed of mono and triglycerides, propylene glycol and water were developed, characterized, and their transformation into gels as well as their ability to prolong the release of incorporated compounds was studied *in vitro* and *in vivo*. After formulation optimization, efficacy was demonstrated in a conditioned place preference model in comparison with daily administration of naltrexone solution.

2. Material and methods

2.1. Material

Propylene glycol (PG), naltrexone hydrochloride and phosphate-buffered saline (PBS) were obtained from Sigma-Aldrich (St. Louis, MO). Monoolein was kindly donated by Kerry (Norwich, NY, USA), and tricaprylin, by Abitec Corporation (Janesville, WI, USA). Acetonitrile, ethanol and methanol were purchased from Mallinckrodt Baker (Phillipsburg, NJ, USA). Alexa fluor 647 was obtained from Thermofisher scientific (Waltham, MA USA).

3. Methods

3.1. Formulation development and phase diagrams

Phase behavior of samples was investigated by mixing various ratios of the structure-forming monoglyceride (monoolein, MO) with propylene glycol (PG), water and tricaprylin; the later was included as oil phase of the microemulsion to enable hexagonal phase obtainment at room and biologically relevant temperatures (Amar-Yuli and Garti, 2005). A MO:tricaprylin ratio of 9:1 (which, for the sake of simplicity, will be referred to as MT) was selected because it has been demonstrated to form the hexagonal mesophase upon a wide range of aqueous content (Amar-Yuli and Garti, 2005), and the influence of propylene glycol (PG) on the phase behavior was assessed. PG was included to aid drug solubilization and reduce the viscosity of the precursor microemulsion, facilitating subcutaneous administration (Phelps et al., 2011). MT and PG were mixed at 9:1 to 2:8 ratios (w/w), followed by addition of water (10–80%). The resulting formulations were visually inspected for transparency, phase separation and fluidity, and visualized under a polarized light microscope (Carl Zeiss, Oberkochen, Germany) for assessment of phase behavior.

3.2. Formulation selection and characterization

Two precursor microemulsions were selected for further characterization: MT:PG:H_2O at 55:25:20 and 65:15:20, which will be referred to as M − 55 and M − 65, respectively. The influence of temperature on the structure of formulations containing water at 20 (microemulsion), 40 and 80% (which formed gels) was evaluated by sample incubation at 37 °C in closed vials maintained in water bath for 30 min, followed by polarized light microscopy. Internal phase diameter of the microemulsions was determined using Zetasizer nanoZS90 equipment (Malvern, Westborough, MA) at room temperature without dilution (due to phase transformation).

The rheological behavior of the microemulsions and hexagonal phase gels (formed after addition of water to obtain a final content of 40%) was investigated using a R/S Plus controlled stress rheometer with the RC75-1 geometry (Brookfield Engineering laboratories, Middleboro, MA) and a water bath circulator for temperature control (25 °C). The experiments were performed with shear rates varying up to 500 s^{-1}. The relationship between shear stress and rate for each formulation was evaluated using the Power law equation (1) $\tau = K \gamma^n$, where τ is the shear stress, γ is the rate of shear, K is the consistency index and n is the flow index (Hosmer et al., 2013; Mahdi et al., 2011).

To evaluate the influence of drug incorporation, naltrexone was added to the selected microemulsions (it was dissolved in PG prior to its mixing with MT) at 1, 5 and 10% (w/w). Additional water was included in the microemulsion to obtain gels with a final aqueous content of 40, 60 or 80% (w/w); subsequently, samples were left to equilibrate for 3 days at room temperature in closed vials before characterization by visual inspection and polarized light microscopy.

3.3. Swelling studies

Swelling studies were performed to compare the rate and kinetics of water absorption and formation of hexagonal phase gels by M − 55 and M − 65. The microemulsions were placed (100 mg) in microcentrifuge tubes, excess water (1 mL) was carefully placed on top of the formulations (dropwise addition to the wall of the top part of the tubes), and the samples were incubated at 37 °C in water bath for 1–48 h. At pre-determined time intervals, water was removed from the vials (its excess was wiped from the tube walls using cotton tips) and they were weighed to determine the amount of water absorbed, which was plotted as function of time and fitted using the first-order kinetic equation (2) $\ln W\infty/(W\infty - W) = kt$, or second-order order equation (3) $t/W = 1/k\, W\infty^2 + t/W\infty$, where $W\infty$ is the maximum water uptake, W is the

water uptake at time *t*, and $W\infty$ - *W* is the unrealized water uptake and *k* is the rate constant (Chang and Bodmeier, 1997; Lara et al., 2005). The rate of swelling was determined by plotting the difference of swelling at two consecutive time points as function of time. To assess the amount of time necessary for hexagonal phase formation, formulations from an additional set of tubes subjected to the same swelling procedure were visualized under a polarized light microscope at 0–24 h.

3.4. In vitro drug release studies

The *in vitro* release of naltrexone from the formulations was evaluated using Franz diffusion cells (diffusion area of 1.77 cm^2; Hanson, Chatsworth, USA) and phosphate-buffered saline (100 mM, pH = 7.2, 7 mL) as receptor phase under constant stirring (350 rpm) at 37.0 ± 0.5∘C. The high solubility of naltrexone hydrochloride in water (50 mg/mL according to the manufacturer) ensures that the entire drug dose added to the donor compartment can dissolve in the receptor phase, and thus, drug release should not be influenced by solubility issues as often observed for non-polar drugs (Carvalho et al., 2017b). A cellulose membrane (cutoff 1000 Da, Sigma, St Louis, MO) was placed between the receptor and donor compartments, and the microemulsions or the control solution (in propylenglycol) were added to the donor compartment of each diffusion cell by transferring the volume equivalent to 100 mg of formulation. To establish the volume equivalent to 100 mg of each formulation, the relationship between mass and volume was determined by weighing (10 times) specific volumes of the formulations as previously described (Carvalho et al., 2017b; Mojeiko et al., 2019); it varied from 104 to 120 μL depending on the formulation.

Contrary to the BRIJ-based formulation previously studied by our group for naltrexone release (which dissolved in contact with the receptor phase within 96 h) (Phelps et al., 2011), the hexagonal phase studied here equilibrated with excess of water, enabling the *in vitro* release to be studied for 120 h. Longer periods could not be studied because of water evaporation and formation of air bubbles in the receptor phase, precluding its contact with the formulation. Aliquots of 200 μL of the receptor phase were collected at 4, 8, 12, 24, 36, 48, 60, 72, 96 and 120 h post-application for drug quantification. Transformation of the precursor microemulsions into hexagonal phase gels occurred during the release study; gels could be observed in the donor compartment within 8 h.

Naltrexone release was quantified by UV-spectrophotometry at 220 nm using standard solutions in the range of 2–100 μg/mL. To estimate cumulative drug release, the amount of drug collected at earlier time points were added to the observed (or measured) drug amount in the receptor phase at a given time point as follows (equation 4):

$$Ct_n = C_n + C_{w,}$$

where Ct_n is the corrected drug amount at a given time n, C_n is the observed drug amount in the receptor phase at a given time n, and C_w is the sum of all drug amounts withdrawn (i.e., collected at earlier time points) (Carvalho et al., 2019b). The release kinetics was determined by plotting cumulative drug release against time (zero order), square root of time (Higuchi), and the log of remaining drug against time (first order), and coefficients of determination were obtained (Migotto et al., 2018; Ng et al., 2017). Based on drug release, M − 55 was selected for further studies.

3.5. Stability screening

Two short-term methods were conducted to estimate the stability of the selected microemulsion (M − 55): centrifugation-based screening and formulation storage at 25 °C for 6 weeks. The unloaded and naltrexone-loaded M − 55 (with 5 and 10% of drug) was subjected to centrifugation at 2000xG at room temperature (Universal 320, Hettich, Tullingen Germany) for 30 min as previously described (Carvalho et al., 2017b). A second set of these samples was stored at 25 °C (temperature maintained by air conditioning) in closed vials, protected from light for 6 weeks. The formulations were assessed macroscopically for creaming, sedimentation and phase separation, as well as microscopically for isotropy and phase transformation (Leica, Wetzlar, Germany). Droplet diameter was assessed using Zetasizer NanoZS90 equipment (Malvern, UK) as described in the item "*Formulation selection and characterization*". To evaluate whether M − 55 would still be able to give rise to hexagonal phase gels after centrifugation or storage for 6 weeks, water was added at a final content of 40%, and the formed gel was inspected by polarized light microscopy.

3.6. Irritation potential

To gather information regarding the irritation potential of the components of the selected microemulsion (M − 55) to the injection site prior to its *in vivo* administration, we assessed production of interleukin-1α (IL-α) and viability of engineered skin equivalents (MatTek Corporation) as endpoints of irritation. Instead of treating the stratum corneum of the tissue as generally performed for topical formulations, the viable layers of the tissue were exposed to M − 55 by treating the culture medium with 50 μL of the microemulsion. By placing M − 55 in contact with the culture medium, we enabled swelling but avoided blocking the contact of the medium with the tissue, which could prevent tissue feeding and decrease viability. We acknowledge the differences between these equivalents and the subcutaneous tissues, but this model better simulates the complex structure of the subcutaneous tissue and the cellular cross talk compared to cells in monolayer, and allows a reduction in animal use. The tissues were incubated at 37 °C and 5% CO_2 for 2, 5 and 18 h; phosphate buffered saline (PBS, negative control) and Triton-X100 (considered a moderate irritant, final concentration of 1% in the culture medium) were used as negative and positive controls, respectively (Bagley et al., 1999; Hosmer et al., 2013; Verhulst et al., 1998). The time intervals were selected based on the "MTT effective time-50 (ET-50) protocol", provided by MatTek, which has been used in other studies from our group (Hosmer et al., 2013).

The culture media were collected at 2–18 h for quantification of extracellular IL-1α using ELISA (Invitrogen, Camarillo, CA, USA). MTT assay was used to account for tissue viability at the last time period: tissues were rinsed with PBS and incubated with 300 μL of MTT solution (1 mg/mL) for 3 h at 37 °C and 5% CO_2, followed by its extraction by immersing the tissues in 2 mL of extraction solution overnight (Hosmer et al., 2013). The optical density of the extracted samples was determined at 570 nm (background reading at 650 nm was subtracted from the readings).

3.7. Animals

Male C57-BL mice from the facility for mice production at the Department of Pharmacology, Institute of Biomedical Sciences were housed in the Animal Facility of the Department of Pharmacology with free access to food and water until they reached 60 days and 25–28 g. The animal room was kept under a 12:12 h light–dark cycle (lights on at 7:00 am), and temperature was maintained between 22 and 23 °C. The protocol was conducted in accordance with guidelines issued by the Brazilian Council for Control of Animal Experimentation (CONCEA), and approved by the Animal Care and Use Committee of the Institute of Biomedical Sciences at University of São Paulo. Experiments were conducted between 7:00 am and 3:00 pm.

Animals were anaesthetized with isoflurane (5% for induction and 2.5% for maintenance, Cristalia, Itapira, Brazil), and the back hair was removed using a depilatory cream applied for 50 s. The cream was rinsed with warm water (32 °C) and the animals were placed at an environmental chamber at 29 °C for recovery from anesthesia. Twenty-

four hours after hair removal, animals were divided in groups based on the treatment they were going to receive as described in the subsequent sessions.

3.8. In vivo subcutaneous administration, hexagonal phase formation and release of a fluorescent marker

This experiment aimed at assessing whether (i) the selected microemulsion (M − 55) transformed into the hexagonal phase gel *in vivo*, (ii) how long after microemulsion administration the gel was formed, and (iii) its ability to prolong the release of a fluorescent marker (Alexa fluor 647) compared to a simple solution. The Alexa fluor-loaded M − 55 (0.05%, w/w) was obtained by dilution of the marker in the polar phase of the formulation; at the concentration employed, the marker did not preclude hexagonal phase formation. A solution of the marker in propylene glycol (0.05%) was prepared for comparison. To ensure that fluorescence was related to the presence of Alexa fluor in the tissue, the unloaded ME-55 was preliminarily administered as control, and did not result in any staining.

Animals were divided in 2 groups that received Alexa fluor solution or Alexa fluor-loaded M − 55. The formulations (100 mg) were administered subcutaneously to the back of the animals, and whole body animal imaging was used to track fluorescence distribution after 1 h, 2, 5, 10, 15, 20 and 34 days using a whole body bioimaging system (IVIS Spectrum System, Perkin-Elmer Life Sciences, Waltham, MA, USA). The following instrument settings were fixed for comparison among groups: exposure time = 5 s, binning factor = 8, excitation/emission = 465/540 nm.

At the end of the experiment, animals were euthanized (thiopental i.p., 200 mg/Kg), and the formulation depot formed in the subcutaneous tissue was removed and visualized under a polarized light microscope to assess whether the hexagonal phase was formed. A separate group (n = 3) of animals was also euthanized 24 h after administration to assess gel formation at a shorter period of time.

3.9. Evaluation of formulation efficacy in the conditioned place preference paradigm

The conditioned place preference (CPP) paradigm is a standard preclinical behavioral model to assess rewarding and aversive drug effects (Cunningham et al., 2006). It was employed to assess whether one dose of M − 55 had comparable effects to daily injections of naltrexone solution in modulating animal response to the rewarding effects of ethanol.

3.9.1. Conditioned place preference paradigm

The assay was conducted using a three-compartment chamber (EP156 C, Insight, Brazil, with dimensions of 4,6 x12,7 × 12,7 cm). The experimental protocol consisted of one habituation session, eight conditioning sessions, and a test session:

- Habituation: in the first day, animals were given an injection of saline. After being returned to the home cage for 1 min, they were positioned at the center of the apparatus for 30 min with free access to all compartments to allow habituation to the apparatus, eliminating novelty as a confounding variable. Baseline data was determined as the average amount of time spent in each chamber. No preference for one compartment over the other was observed, and the apparatus was considered unbiased.
- Conditioning (days 2–9): four ethanol pairings (i.p., 2 g/kg) were alternated with four saline pairings. Within each experimental group, animals were dosed in different compartments: half of the animals received ethanol or saline in the black/rod floor compartment and half in the white/mesh floor compartment. Also, animals received saline or ethanol in alternate days. Upon placement into the CPP apparatus, mice had access to only one of the conditioning compartments, and after entering this compartment, the guillotine door was closed and they were confined for 5 min.
- Test (day 10): no drug or vehicle was administered on the test day; animals were placed into the central compartment and given free access to all compartments for 30 min. The test sessions were recorded and the amount of time that the animals spent in each compartment was measured by an experimenter blind to the group allocation.

CPP was evaluated by comparing the amount of time spent in the ethanol-paired compartment during habituation (H) and on day of the test (T) according to the equation (5): $\Delta t = tT\text{-}tH$, where tT and tH represent the amount of time spent in the compartment paired with ethanol on the test (post-conditioning after ethanol treatment) and habituation day (pre-conditioning before ethanol treatment), respectively.

3.9.2. Treatment and assessment of formulation efficacy

Animals were divided in 5 groups according to the treatments they were going to receive:

- Group 1 (CT-S): saline (s.c., 1 mg/Kg daily)
- -Group 2 (CT-NTX): naltrexone solution (s.c.,1 mg/Kg daily)
- Group 3 (M − 55%): unloaded formulation (s.c., 100 mg/animal, one dose)
- Group 4 (M − 55 5%): M − 55 containing naltrexone at 5% (s.c., 100 mg/animal, one dose)
- Group 5 (M − 55 10%): M − 55 containing naltrexone at 10% (s.c., 100 mg/animal, one dose)

During the conditioning phase, groups 1 and 2 received daily injections of saline and naltrexone, respectively, 30 min before ethanol administration, whereas groups 3–5 received one dose of M − 55 (unloaded or containing naltrexone at 5 or 10%), on the first day of conditioning.

To establish relationships between differences in animal behavior after the various treatments and naltrexone plasma levels, the drug was quantified in the plasma at the end of the efficacy test. Animals were anesthetized with ketamine-xylazine (100 mg/Kg e 10 mg/Kg, i.p.), and blood was withdrawn by inferior vena cava puncture prior to euthanasia. Plasma was prepared by centrifugation of blood samples at 4000xg for 10 min and stored at − 80 °C. For naltrexone extraction, 120 μL of plasma was mixed with 10 μL of NaOH and 500 μL of ethyl acetate, vortexed for 1 min, centrifuged (4000xg) for 5 min, and the supernatant was collected and dried. The residue was suspended in the mobile phase, and analyzed by HPLC. Using this method, naltrexone recovery from plasma samples varied within 79–88%.

Chromatographic analyses were performed using a Shimadzu HPLC system equipped with a pump (model LC-20AB), an autosampler (model SIL-20A), an UV detector (model SPD-M20A) set at 215 nm, and the Class-VP software. Naltrexone separation was performed in a Phenomenex C18 (150 × 4.6 mm) column maintained at 25 °C, using a mobile phase composed of 7:3 (v/v) acetonitrile:water (acidified with 0.005% phosphoric acid) at a flow rate of 1.0 mL/min. Calibration solutions of naltrexone were prepared in acetonitrile and plasma (drug was extracted as described earlier in this topic), and demonstrated linearity within the range 0.05–50 μg/mL (for acetonitrile solutions) and 0.06–10 μg/mL (for curves extracted from plasma). The limit of detection of the method was 0.035 μg/mL. The amount injected into the column was 20 μL for samples and calibration solutions. For each experiment, new calibration curves were obtained.

3.10. Statistical analysis

The results were reported as means ± standard deviation or means ± standard error (as denoted in each figure caption). Data from

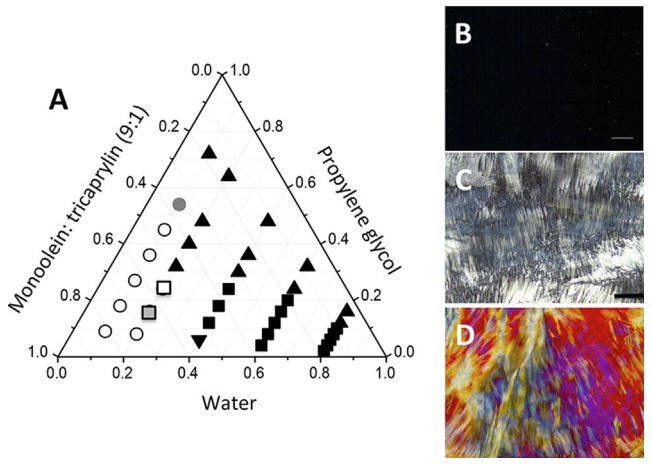

Fig. 1. Relationship between composition and phase behavior of samples composed monoolein, tricaprylin, propylene glycol (PG) and water. A: pseudo-ternary phase diagrams; monoolein and tricaprylin at 9:1 (w/w) were mixed with PG at ratios varying from 9:1 to 2:8 (w/w), and water was added at 10–80%. M−65 and M−55 are depicted as gray and white squares, respectively, in the diagram. White circles: isotropic, single-phase fluids, characterized as microemulsions; inverted triangles: hexagonal phase; black squares: hexagonal phase + excess water; triangles: two-phase systems; grey circle: transition. B: polarized light microscopy image of M−55; C: polarized light microscopy image of M−55 containing water; D: polarized light microscopy image of M−65 containing water.

swelling studies were statistically analyzed using one-way ANOVA (followed by Tukey post-hoc test, GraphPad Prism software), whereas analysis of data from the *in vitro* release studies was performed using repeated-measures ANOVA (followed by Fisher post-hoc test, Statistica Advanced 8.2 software). Values were considered significantly different when $p < 0.05$.

4. Results

4.1. Phase diagrams and formulation selection

Formation of isotropic, single phase and fluid systems (compatible with microemulsions) were observed with water up to 20%; higher concentrations led to fluid two-phase systems or gels, latter classified as hexagonal phases (Fig. 1). The hexagonal phase co-existed with excess water (hexagonal phase + water) with aqueous content at 40% or above, and PG content at 25% or lower. This phase existed at narrower aqueous contents as PG concentration increased, and could uptake less water. At MT:PG ratios lower than 4:6, hexagonal phase formation was precluded, and only microemulsions or two-phase systems were observed. This is not unexpected, since PG replaces the content of the structure-forming lipid (monoolein), hindering the formation of liquid crystals as reported for other surfactant-based systems (Phelps et al., 2011).

Microemulsions formed with MT:PG:H_2O at 55:25:20 and 65:15:20, w/w were selected for further studies (M−55 and M−65, respectively) because they (i) transitioned into hexagonal phases upon uptake of small additional water amounts, and (ii) contain different PG contents; due to PG influence on viscosity and drug release, this comparison offers the opportunity to select the formulation with the most desirable release rate. Their composition is represented in Fig. 1**A** as white and grey squares. A polarized light photomicrograph of M−55 is depicted in Fig. 1**B**, demonstrating that the formulation is isotropic, and no specific texture could be observed under the microscope**;** a similar texture was observed for M−65 (not shown). Addition of water (to a final content of 40%) to M−55 and M−65 gave rise to hexagonal phase gels with little excess water (Fig. 1**C-D**). No alterations in the structures

Table 1
Physicohecmical characteristics of selected microemulsions, and coefficients of determination for the formulations swelling and naltrexone release. Data represented as average ± standard deviation, n = 3–8 depending on the experiment.

Unloaded formulation	Physicochemical characteristics		Swelling (r^2)			Drug (%)	Release (r^2)	
	Size (nm)	PDI	Zero order	First order	Second order		Zero order	Square root of time	First order
M−55	35.3 ± 3.1	189.5 ± 10.9	0.320 ± 0.001	0.747 ± 0.105	0.870 ± 0.086	0.993 ± 0.013	M−55 5%	0.917 ± 0.021	0.995 ± 0.018	0.946 ± 0.017
M−65	30.0 ± 1.8	165.2 ± 19.5	0.340 ± 0.003	0.504 ± 0.102	0.868 ± 0.092	0.990 ± 0.009	M−65 5%	0.939 ± 0.028	0.991 ± 0.008	0.907 ± 0.031
							M−55 10%	0.904 ± 0.034	0.968 ± 0.020	0.843 ± 0.034

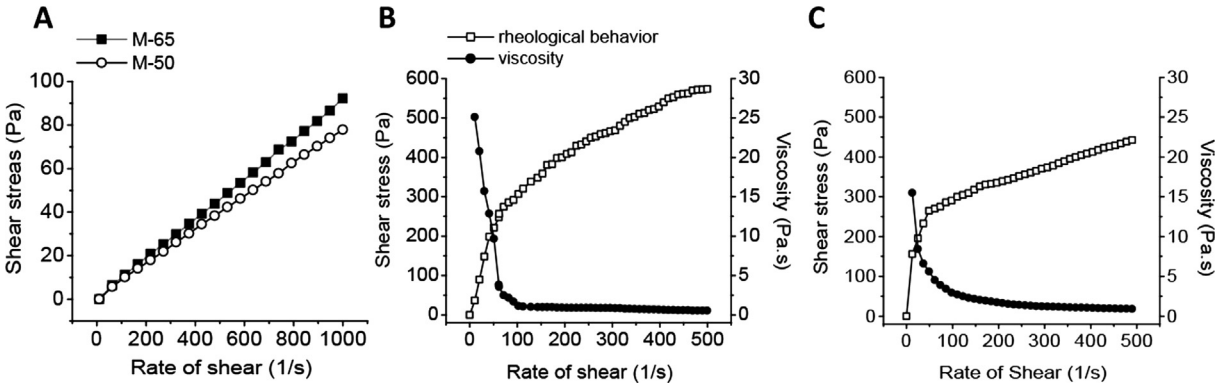

Fig. 2. Rheological behavior and viscosity of microemulsions and their gel counterparts containing water. A: microemulsions, B: M−65 with water (40%), C: M−55 with water (40%).

of these formulations were observed after their incubation at 37 °C, suggesting that the hexagonal phase would be formed at biologically relevant temperatures.

4.2. Microemulsion characterization and swelling

As can be observed in Table 1, light scattering analysis evidenced the existence of two populations, with the higher frequency population depicting diameter of ~ 165 and 190 nm (see Supplementary Fig. 1 for a representative size distribution diagram); as a result, the polydispersity index (PDI) was 0.32 and 0.34, which denotes medium polydispersity (Carvalho et al., 2019b; Loureiro et al., 2015). The existence of more than one droplet population has been previously reported in microemulsions (Holmberg et al., 2004; Laia et al., 1998).

The flow properties of these microemulsions and their respective hexagonal phase gels (obtained with water at 40%) are displayed in Fig. 2. Both microemulsions displayed Newtonian behavior, characterized by linear relationships between shear rate and stress, and flow index close to 1. Their viscosity, calculated as the average of viscosity at individual rates of shear, were 0.105 and 0.083 Pa.s for M−65 and M−55, respectively, demonstrating that M−65 is ~ 1.3-fold more viscous, and the microemulsions were 2–2.3-fold more viscous than propylene glycol. The behavior of the hexagonal phase gels was consistent with pseudoplastic systems, characterized by a non-linear relationship between shear rate and stress and a decrease in viscosity (shear-thinning behavior) as the rate of shear increased. This classification was further supported by values of the flow index below 0.7. The gel formed by M−65 was more viscous, as demonstrated by the increased shear stress necessary to generate the same rate of shear compared to M−55.

The rate and kinetics of water uptake by the microemulsions were determined through two parallel studies: one was conducted by gravimetric determination of water absorbed and the other, by assessment of hexagonal phase formation by polarized light microscopy. The water uptake percentage and rate are demonstrated in Fig. 3**A and B**. Both microemulsions quickly absorbed water, and at approximately 8 h, they reached their respective equilibrium concentration. At the end of the time window studied, M−65 and M−55 were capable of absorbing 19.0 ± 2.0% and 15.1 ± 2.2% of water, respectively. The maximum rate of water uptake was achieved after 1 h for both microemulsions (Fig. 3**B**), denoting similarities in the uptake process.

Fig. 3**C** depicts polarized light microscopy images of the microemulsions after 0, 4, 8 and 24 h of contact with water. At 0 h, both formulations were liquid, clear isotropic phases, consistent with their classification as microemulsions. After 4 h of contact with water, it was possible to note signs of anisotropy (and thus, phase transformation) especially in M−65. This difference might result from the higher amount of water absorbed by M−65 (as demonstrated in Fig. 3**A**), bringing its aqueous content closer to that necessary for transformation into the hexagonal phase in less time. At 8 h, both microemulsions had transformed into hexagonal phase gels, which continued to exist for at least 2 weeks (last time point assessed).

Data fitting to equations (2) and (3) revealed that swelling can be better described by second order kinetics (with coefficients of determination higher than 0.99, **Table 2**). This was expected, and similar swelling results were described for monoolein and phytantriol-based systems, and even for other surfactant-based formulations, such as BRIJ (Boyd et al., 2006; Fong et al., 2009; Phelps et al., 2011).

4.3. Effect of naltrexone incorporation

Microemulsions M−55 and M−65 containing up to 5% of naltrexone were clear and fluid, whereas those containing 10% were turbid even after bath sonication for 20 min, indicating that part of the drug could not dissolve in the formulation. Addition of water to samples containing 5 and 10% of naltrexone to reach final concentrations of 40 and 80% yielded clear hexagonal phase gels after sample incubation at room temperature or at 37 °C (Supplementary Fig. 2). These results suggest that naltrexone did not preclude hexagonal phase formation at the concentrations studied, and that water uptake aided drug dissolution in the system.

4.4. Naltrexone in vitro release

The *in vitro* release study was performed to compare the two microemulsions and assess how composition affected drug release. When a PBS solution of naltrexone (5%, control) was applied to the donor compartment, larger drug amounts were transported across the membrane compared to both microemulsions during the studied time period (Fig. 4), demonstrating that (i) the membrane did not limit naltrexone diffusion, and (ii) the hexagonal phases resulting from water uptake by both microemulsions can prolong naltrexone release. Comparing the two microemulsions, significantly higher amounts ($p < 0.05$) of naltrexone were released from M−55 from 48 to 120 h, and at 120 h (the latest time point studied), 36.3 ± 5.9 and 22.7 ± 4.1% of drug was released from M−55 and M−65, respectively. Whether this release rate would translate into effective plasma concentration in humans remains to be determined, as crucial *in vivo* aspects related to drug absorption and disposition (that influence drug plasma concentrations) are absent *in vitro*. To establish this type of *in vitro-in vivo* mathematical correlation, a pharmacokinetic study to associate *in vitro* amounts of drug released and *in vivo* plasma levels would be necessary (Andhariya et al., 2017; Davanco et al., 2020).

Increasing the amount of drug from 5 to 10% did not affect the kinetics of drug release (Fig. 4), demonstrating no influence of drug loading on the release process. Regardless of composition differences

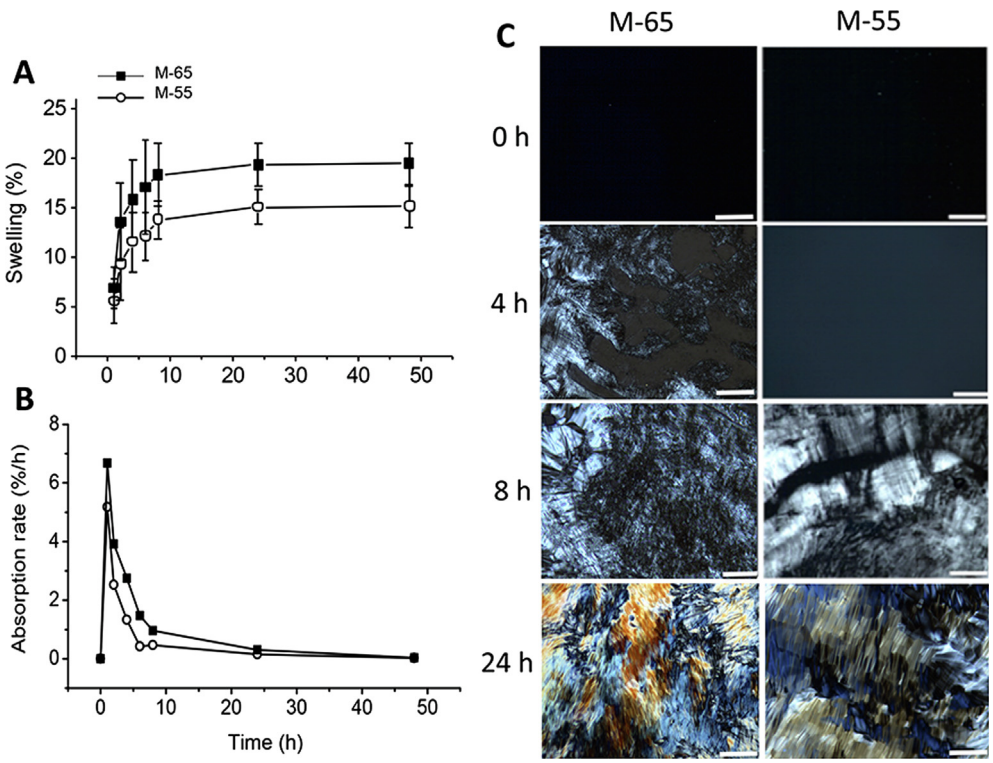

Fig. 3. Water uptake by microemulsions. (A) water uptake by M−55 and M−65 as function of time; (B) rates of water uptake by M−55 and M−65; (C) polarized light microscopy pictures of microemulsions before and after contact with water for 2–24 h, 25 °C. Data shown as means ± standard deviation of 4–6 replicates; scale bar = 200 μm. At 0 h, both microemulsions were isotropic; at 4 h, M−65 depicted signs of transformation into hexagonal phase, and after 8 h, both formulations were transformed into hexagonal phase.

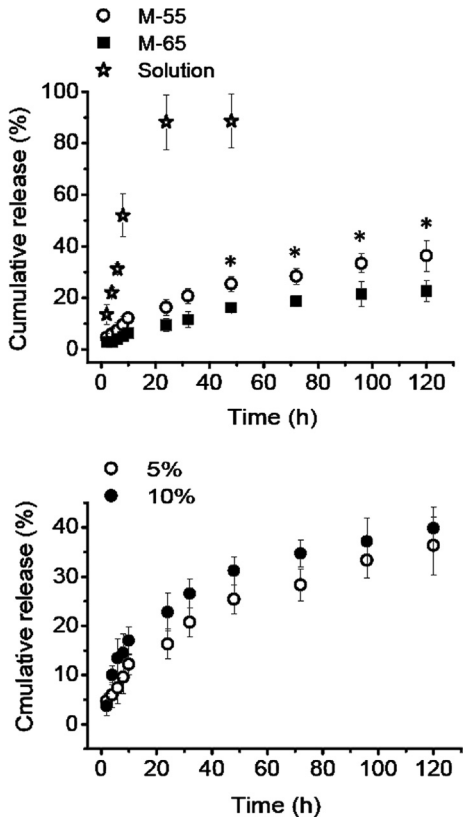

Fig. 4. Cumulative *in vitro* release of naltrexone. (A) release of naltrexone incorporated at 5% (w/w) in microemulsions M−65 and M−55 compared to a drug solution; (B) influence of naltrexone loading on its *in vitro* release from M−55. Each point represents means ± standard deviation of 4–6 replicates. *p < 0.05 compared to M−65.

between M−55 and M−65, release was proportional to the square root of time, as demonstrated by the higher values of the coefficient of determination obtained by fitting the data to the various kinetics models (Table 1). M−65 and M−55 containing either 5 or 10% of naltrexone formed a clear gel in the donor compartment within 8 h; thus, it is reasonable to assume that M−55 containing 5 or 10% of drug displayed similar characteristics along the majority of the *in vitro* release study, and that the results express the release properties of M−55 containing the dissolved drug. This is further supported by the release kinetics observed, which suggests that drug release is controlled by diffusion and not by the rate of drug dissolution (Chandrasekaran and Paul, 1982; Helledi and Schubert, 2001).

Because M−55 released approximately 1.5-fold more drug than M−65 during the studied period, and drug loading did not affect release kinetics, this microemulsion was selected for further studies.

4.5. Stability screening

No phase separation, transformation or creaming was observed by visual inspection and polarized light microscopy after centrifugation or storage for 6 weeks of the unloaded and naltrexone-loaded M−55 (Supplementary Fig. 3). No pronounced changes on size were observed on the unloaded or naltrexone-loaded M−55 (at 5%, Supplementary Table 1) compared to initial values (depicted in Table 1), suggesting stability. Diameter of M−55 containing naltrexone at 10% was not determined due to the presence of drug particles, which could lead to an erroneous estimation of droplet size. The microemulsions were still capable of forming hexagonal phase gels (upon addition of water to 40%) after being subjected to centrifugation or storage for 6 weeks, indicating that their ability to originate the gels was not altered (Supplementary Fig. 3).

4.6. Estimation of the irritation potential

The irritation potential of M−55 (the selected microemulsion) was compared to that of Triton-X100 and PBS using bioengineered skin as model. Compared to PBS, Triton increased IL-1α release by the tissue at

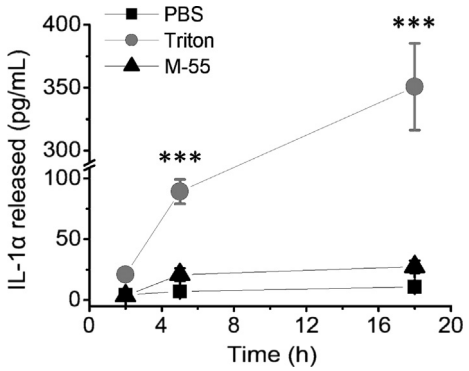

Fig. 5. Time-dependent effects of treatments (PBS, Triton-X100 and unloaded M−55) on the release of IL-1α by bioengineered skin tissues. * $p < 0.05$ compared to PBS, *** $p < 0.001$ compared to PBS. Each point represents means ± standard deviation of 3 replicates.

all time-points studied (Fig. 5), and at the latest time point, the amount of cytokine was approximately 30-fold higher ($p < 0.001$) than after PBS exposure. Considering that IL-1α release was most likely impacted by the low tissue viability (21.1 ± 7.1%), if we normalize cytokine production by the viability of tissues exposed to Triton or PBS, Triton-induced cytokine release would be approximately 150-fold higher. Applying the same rationale for M−55−exposed tissues (whose viability was 72.4 ± 14.8%), cytokine release would be ~ 3.5-fold higher compared to PBS treatment, but approximately 40-fold lower than Triton. These results suggest that M−55 can be considered safer than the moderate irritant Triton, and can be employed in the pre-clinical assay.

4.7. In vivo subcutaneous administration, hexagonal phase formation and release of a fluorescent marker

Fig. 6**A** depicts representative images of animals subjected to subcutaneous administration of M−55 or a solution of the fluorescent marker Alexa fluor 647. Administration of the microemulsion resulted in the formation of a strong fluorescent area at the injection site, and despite the reduction of intensity and dimension of this area over time, local fluorescent staining could still be detected at 20 days post-application. Administration of the control solution also resulted in strong fluorescent staining at the administration site, but fluorescence signals decreased faster and in a more pronounced manner after 5 days compared to the microemulsion. This comparison can be better visualized in Fig. 6**B**, which shows that fluorescence signals decreased slower and in a less pronounced manner within the studied time period in animals treated with M−55.

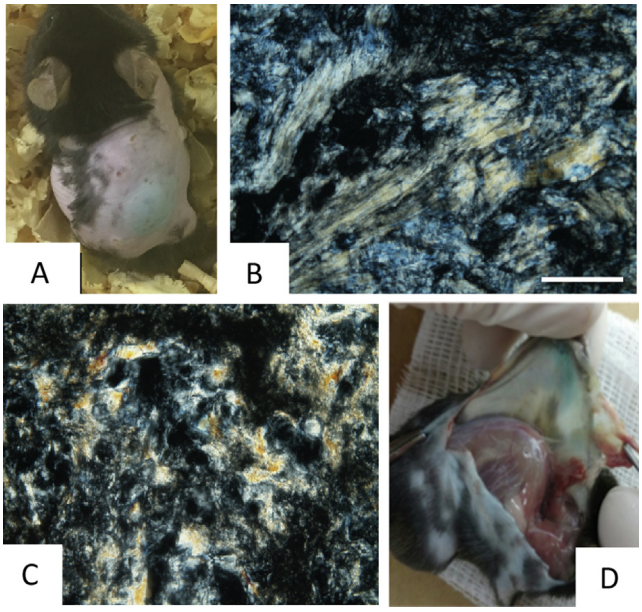

Fig. 7. Formulation administration and *in vivo* hexagonal phase formation. A: animal at 24 h post-administration of M−55, depicting formation of a depot with light blue color due to Alexa fluor incorporation; B: depot observed under polarized light microscopy 24 h after M−55 subcutaneous administration demonstrating hexagonal phase formation; C: depot at 34 days after *in vivo* administration of M−55 demonstrating that the hexagonal structure was maintained; D: subcutaneous tissue 5 days after administration of Alexa fluor solution to show tissue staining.

The area of fluorescence staining in M−55−treated animals correlated with formation of a gel; at 24 h, it was blue in appearance (due to the presence of Alexa fluor) and displayed a fan-like texture compatible with hexagonal phase, demonstrating that *in vivo* formation of the liquid crystalline gel occurred within one day (Fig. 7**A and B**). At

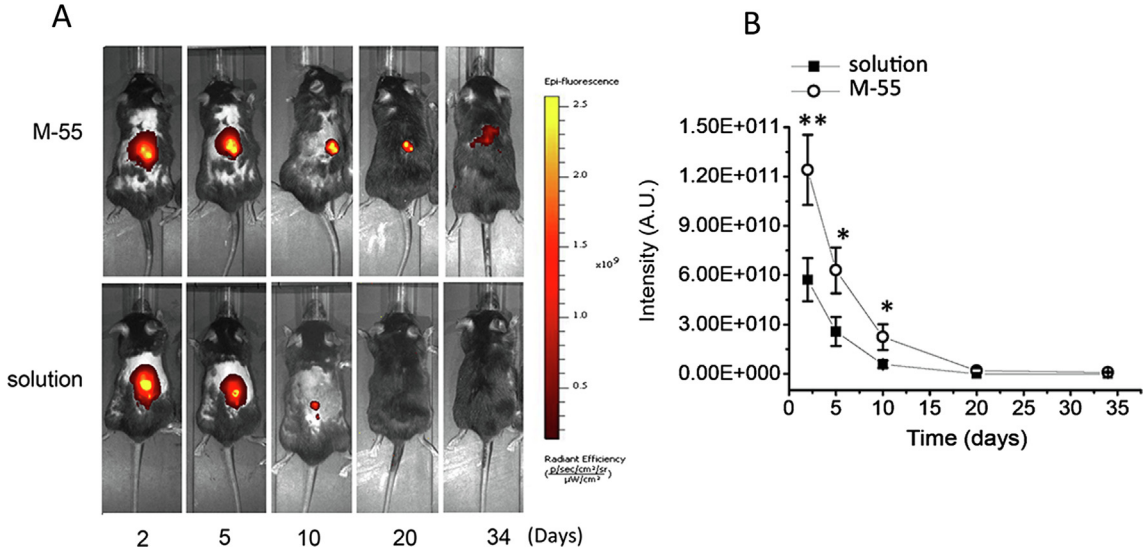

Fig. 6. In vivo retention of the fluorescent marker Alexa fluor administered loaded in M−55 or as a solution in propylene glycol. A: whole animal images showing fluorescence staining after subcutaneous administration of M−55 or the solution; B: local fluorescence intensity decay as a function of time, n = 4–6 animals/group. ** $p < 0.01$ and * $p < 0.05$ compared to Alexa fluor solution.

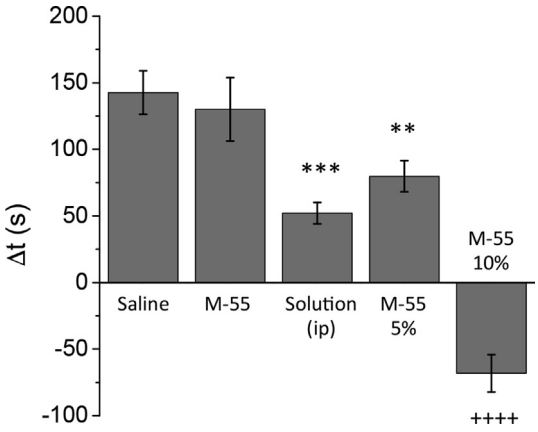

Fig. 8. Influence of naltrexone i.p, (solution) and M−55 (unloaded or containing 5 or 10% naltrexone) on ethanol-induced conditioned place preference (CPP). Data are shown as CPP score (difference in the time spent in ethanol-paired compartment during pre and post-conditioning); average ± standard error of 4–8 animals/group. Treatments: saline, naltrexone solution (5%), unloaded M−55 (M−55), M−55 containing 5% of naltrexone (M−55 5%) and M−55 containing 10% of naltrexone (M−55 10%). ** $p < 0.001$ and *** $p < 0.0001$ compared to saline treatment, $^{++++}p < 0.0001$ compared to saline and naltrexone solution.

day 34, the remaining gel displayed a similar texture (Fig. 7**C**), demonstrating its ability to retain its structure *in vivo*. Even though fluorescence was measurable in animals treated with Alexa fluor dissolved in propylene glycol at day 5, no solution remained locally after 24 h. However, a blue staining was observed at the tissue (Fig. 7**D**), suggesting Alexa fluor adsorption. Thus, the fluorescent signal in animals injected with Alexa fluor solution can be attributed to the presence of the compound adsorbed to the tissue and not of a formulation capable of prolonging release. Tissue staining was not observed in the microemulsion-treated animals, most likely because of the formulation ability to slow down Alexa fluor release, avoiding its interaction and adsorption at the tissue.

4.8. Evaluation of formulation efficacy in the conditioned place preference paradigm

The CPP score of animals treated with a single dose of M−55 containing 5% naltrexone was significantly lower ($p < 0.01$) than control animals (Fig. 8), demonstrating the efficacy of the formulation in reducing place preference. This effect depended on the presence of naltrexone, since injection of the unloaded formulation resulted in a score similar to the control. There was no significant difference comparing Δt in the group treated with a single dose of the microemulsion and daily injections of naltrexone solution, demonstrating the advantage of the microemulsion containing 5% of naltrexone in terms of reducing the frequency of administration. On the other hand, animals treated with M−55 containing 10% of naltrexone showed a significant decrease ($p < 0.0001$) in CPP score compared to saline, naltrexone solution i.p. and M−55 5% groups, suggesting that the high dose of naltrexone induced aversion to the ethanol-associated compartment.

To try to correlate animal behavior and naltrexone plasma concentrations, drug quantification was performed at the end of the test. It is worth noting that our goal was not to determine pharmacokinetic parameters or perform a comprehensive PK/PD study, but to investigate whether the difference in CPP behavior induced by M−55 containing 10% naltrexone was associated with higher plasma concentrations. Naltrexone concentration was below the limit of quantification of the method (0.06 μg/mL) in animals treated with one dose of M−55 containing 5% of naltrexone, although a small peak close to the limit of detection could be observed, and increased to 0.072 ± 0.035 μg/mL in animals treated with M−55 with 10% naltrexone, demonstrating that plasma concentration increased with drug content in the formulation. Naltrexone plasma concentrations > 2 ng/mL are necessary for the effect (Verebey et al., 1976). Because treatment with M−55 with 10% of naltrexone resulted in higher drug levels at the end of the CPP study, we can assume that the amount of drug released was sufficient to generate effective concentrations and the pharmacological effect observed in the pre-clinical model. Whether the release rate provided by M−55 would be sufficient for efficacy in humans remains to be determined.

5. Discussion

Formation of liquid crystalline phases can be brought about by thermal processes (forming thermotropic phases) or by the addition of solvents (forming lyotropic phases) (Stevenson et al., 2005); our goal was to obtain gels in response to the uptake of fluids from biological tissues. When exposed to water, both M−55 and M−65 gave rise to hexagonal phases *in vitro* within 8 h, reaching equilibrium upon absorption of 15–19% of water. This is consistent with the phase behavior depicted in the diagram of Fig. 1, which shows transition to hexagonal phase + excess water (after which additional water uptake is not expected) at 40% of water. This result suggests that replacing 10% of MT with propylene glycol in M−65 to obtain M−55 did not substantially hamper its water uptake capacity.

In addition to the aqueous content, other factors are known to influence the phase behavior of monoolein-based samples, including addition of other compounds and temperature. The influence of other compounds can be exemplified by tricaprylin, employed here to enable formation of the hexagonal phase at biologically relevant temperatures (Amar-Yuli and Garti, 2005; Norling et al., 1992). Medium chain triglycerides are capable of solvating the tails of monoolein, affecting its critical packing parameter, and transforming the lamellar or cubic phases into hexagonal mesophases (Amar-Yuli and Garti, 2005). Similarly, interactions between naltrexone and the polar headgroup of monoolein may be possible, affecting the interfacial curvature, water uptake and phase formation, as demonstrated previously when cyclosporine was included in monoolein-based systems (Caboi et al., 2001; Lopes et al., 2006). Our results suggest that naltrexone neither precluded hexagonal phase formation nor induced formation of other systems independently on drug concentration and state (dissolved or dispersed) up to 10%. Similar observations were reported for BRIJ-based liquid crystalline phases with naltrexone up to 5% (Phelps et al., 2011).

Consistent with other microemulsions, both M−55 and M−65 displayed Newtonian behavior, which can be considered an advantage since the force necessary for injection will be affected by the injecting speed and formulation viscosity; since viscosity remains constant during shearing, its influence is more easily controlled (Allahham et al., 2004; Carvalho et al., 2017a; Carvalho et al., 2019b). On the other hand, the hexagonal phase gels displayed pseudoplastic behavior, which may be related to the formation of multilamellar vesicles at high rates of shear (Carvalho et al., 2010; de Silva et al., 2011; Junqueira Garcia et al., 2018). Because M−65 was more viscous at lower shear rates, it is reasonable to suggest that drug diffusivity was reduced, justifying naltrexone slower *in vitro* release (Hosmer et al., 2013; Makai et al., 2003; Pepe et al., 2013). These results support the influence of MT and PG content, with an increased release being observed as the initial content of the structure-forming compound decreased and PG content increased (Junqueira Garcia et al., 2018; Lara et al., 2005; Makai et al., 2003). A similar effect was reported due to a decrease in surfactant content in BRIJ-based gels and in microemulsions (Hosmer et al., 2009; Phelps et al., 2011).

Drug solubility has been recognized as an important factor influencing the rate and extent of release from swellable matrices, and developing prolonged release devices for water-soluble drugs like

naltrexone hydrochloride is generally considered a challenge (Li et al., 2008). Hydrophilic polymer matrix systems, which have been widely employed to modulate drug release (specially oral), often enable rapid diffusion of water-soluble drugs through the gel network, increasing the risk of toxic concentrations (Yadav et al., 2012). To prolong the release of hydrophilic drug, hydrophobic excipients have been included in hydrophilic matrices and gels. Malonne et al. (Malonne et al., 2000) demonstrated that monoolein-based systems containing fatty acids provided a slower *in vitro* release of tramadol hydrochloride, and prolonged its analgesic activity in the rat tail flick test, showing analgesia for over 10 h compared with the 3–4 h obtained with the drug solution. Thus, addition of the triglyceride tricaprylin in the monoolein-based hexagonal phase might have been important to prolong naltrexone release.

The components of M − 55 were considered safer than a moderate irritant (Triton), as demonstrated by a lower release of IL-1α and higher tissue viability, which indicated the feasibility of employing the formulation in the pre-clinical assay. One limitation of the assay as it was employed here was that it only enabled a comparison of the formulation with controls. Although the use of bioengineered skin models is well accepted to estimate the irritation potential of topical formulations (Faller et al., 2002; Semlin et al., 2011), it has not been validated (and specific endpoints have not been set) for parenteral formulations, and thus, a combination of *in vitro* and *in vivo* assays is most likely necessary to ensure the safety of M − 55 prior to clinical use. Another limitation of this assay is that it did not address the effect of water uptake and gel formation within the tissue, since the gel was formed upon contact with the free culture medium and did not depend on the extraction of interstitial fluid. This is an important factor for local reactions, as demonstrated by Borgheti-Cardoso *et al.* (Borgheti-Cardoso et al., 2015). The authors observed that monoolein-based systems did not alter tissue architecture, but influenced recruitment of inflammatory cells; after 7 days, a granulation tissue was observed at the site of injection, and after 14 days, tissue repair took place (Borgheti-Cardoso et al., 2015). Since monoolein is considered nontoxic (Ganem-Quintanar et al., 2000), these effects were attributed to the pressure exerted on the surrounding tissue due to the *in situ* gel formation rather than chemical tissue damage (Borgheti-Cardoso et al., 2015). Nevertheless, it is worth mentioning that weight loss or difficulty in locomotion was not observed in M − 55 − treated animals, suggesting that its injection did not affect the overall animal well-being.

Subcutaneous injection of M − 55 led to formation of a gel with hexagonal structure and slower release of the fluorescent marker Alexa fluor compared to a solution, and after 20 days, fluorescence could still be detected at the site of injection. This was consistent with the persistence of the gel, whose remains was observed until day 34, and confirms previous reports concerning the time necessary for gel removal from the tissue (Borgheti-Cardoso et al., 2015). Additionally, unlike the solution, M − 55 ability to slow down Alexa fluor release prevented its adsorption in the subcutaneous tissue and in the skin. This is an interesting result, since undesirable drug accumulation in tissues might lead to toxic reactions and other pharmacological effects (Sakaeda et al., 2018).

Compared to the BRIJ-based system that we have previously studied (Phelps et al., 2011), M − 55 can be considered more advantageous since it (i) resisted dilution *in vitro* and *in vivo*, as observed by the persistence of the gel *in vitro* for 2 weeks and for 34 days after subcutaneous administration, (ii) enabled incorporation of 10% of naltrexone, twice the amount suspended in BRIJ-based systems, and (iii) promoted a slower drug release. In theory, these characteristics point to the possibility to administer larger amounts of naltrexone that would be subjected to prolonged release for longer periods of time, which could potentially reduce the frequency of administration.

The efficacy of M − 55 containing 5% naltrexone was demonstrated by a reduction in the CPP score during the test. Its efficacy was similar to daily drug injections, which demonstrates that M − 55 enables a reduction on dosing frequency, and thus, may contribute to improve patient compliance to treatment. Increasing naltrexone concentration in M − 55 to 10% resulted in a more robust effect, compatible with place aversion. It has been previously observed that aversion may occur as function of naltrexone dose, the addictive drug dose, and the interval between them (Parker and Rennie, 1992; White et al., 2005). Verebey *et al.* demonstrated that plasma levels > 2 ng/mL are necessary to antagonize the effect of 25 mg intravenously administered heroin (Verebey et al., 1976), and doses used for treatment of patients with alcohol addiction generally produce steady-state plasma concentrations of naltrexone ranging between 3 and 40 ng/ml (Brunen et al., 2019). M − 55 with 10% of drug produced plasma concentrations above this range (which was reasonable to expect since drug loading did not impact the release kinetics) and might justify the aversive behavior. Although aversion is often considered a limiting factor for treatment adherence (Friedmann et al., 2013), the level of naltrexone-induced aversion has been demonstrated to predict subsequent reduction in ethanol consumption, especially in patients that actively consume high levels of alcohol (Mitchell et al., 2009).

6. Conclusion

In conclusion, microemulsions capable of transitioning into gels with hexagonal structure *in vivo* were characterized and optimized. M − 55 (the selected microemulsion) was easy to prepare, resisted for over 30 days in the subcutaneous tissue, and allowed incorporation of naltrexone at a wide range in a dissolved or suspended form without precluding hexagonal phase formation. This could enable drug loading to be tailored to match patient/treatment needs, providing individualized treatment options while expanding the potential uses of the delivery system to treat other forms of addiction and/or diseases requiring varied doses of naltrexone. For example, low doses of naltrexone have been proposed and studied for long-term treatment of autoimmune disorders, cancer, obesity, prevention of cocaine relapse in association with levo-tetrahydropalmatine and in dermatological disorders (Liu et al., 2016; Sikora et al., 2019; Sushchyk et al., 2016), while, as mentioned earlier, aversive doses may be important for patients that consume high levels of alcohol. Although we presented promising results in terms of formulation pre-clinical efficacy, several questions remain and should be elucidated in future studies. Our results demonstrated that M − 55 enabled a reduction on dosing frequency compared to the solution, which may contribute to improve patient adherence to treatment. However, considering that the formulation remains *in vivo* for over 30 days, further studies regarding how long naltrexone effects could be maintained after a single administration are necessary to estimate the frequency of dosing and whether M − 55 offers advantages compared to other prolonged release formulations. Additionally, future studies should investigate local *in vivo* reactions and compare the systemic adverse effects resulting from naltrexone conventional formulations and M − 55. Although naltrexone-related adverse effects are not usually life threatening (except in patients currently using opioids) (Bolton et al., 2019), reduction of their incidence might aid treatment adherence.

CRediT authorship contribution statement

Rogério A. Santos: Conceptualization, Investigation, Methodology, Formal analysis, Writing - original draft. **Mariana Rae:** Methodology, Investigation. **Vanessa F.M.C. Dartora:** Methodology, Investigation, Formal analysis, Writing - original draft. **Jenyffer K.R. Matos:** Methodology, Investigation. **Rosana Camarini:** Conceptualization, Formal analysis, Supervision, Funding acquisition, Writing - review & editing. **Luciana B. Lopes:** Conceptualization, Supervision, Funding acquisition, Formal analysis, Methodology, Writing - original draft, Writing - review & editing.

Declaration of Competing Interest

The authors declare that they have no known competing financial interests or personal relationships that could have appeared to influence the work reported in this paper.

Acknowledgements

We thank Mr. Moacir F. Brito (MS) for assistance with the HPLC method development, Mr. Pedro F. Ribeiro for early assistance with formulation characterization, and Dr. Alexandre A. Steiner (Instituto de Ciências Biomédicas – Universidade de Sao Paulo) for assistance with the bioimaging experiment. This study was supported by São Paulo Research Foundation (FAPESP, grant# 2013/16617-7, 2015/02397-0, 2018/05038-0 and 2018/13877-1), National Council of Technological and Scientific Development (CNPq, grant# 443549/2014-1 and 408228/2016-4), and PhRMA Foundation. Fellowships from CAPES (finance code 001) and FAPESP (2017/04174-4 and 2018/18813-1) are greatly appreciated. Bioimaging studies were conducted at the CEFAP core facility (Instituto de Ciências Biomédicas – Universidade de Sao Paulo).

Appendix A. Supplementary data

Supplementary data to this article can be found online at https://doi.org/10.1016/j.ijpharm.2020.119474.

References

Al-Tahami, K., Oak, M., Singh, J., 2011. Controlled delivery of basal insulin from phase-sensitive polymeric systems after subcutaneous administration: In vitro release, stability, biocompatibility, in vivo absorption, and bioactivity of insulin. J Pharm Sci 100, 2161–2171.

Allahham, A., Stewart, P., Marriott, J., Mainwaring, D.E., 2004. Flow and injection characteristics of pharmaceutical parenteral formulations using a micro-capillary rheometer. Int J Pharm 270, 139–148.

Amar-Yuli, I., Garti, N., 2005. Transitions induced by solubilized fat into reverse hexagonal mesophases. Colloids Surf B Biointerfaces 43, 72–82.

Andhariya, J.V., Shen, J., Choi, S., Wang, Y., Zou, Y., Burgess, D.J., 2017. Development of in vitro-in vivo correlation of parenteral naltrexone loaded polymeric microspheres. J Control Release 255, 27–35.

Bagley, D.M., Gardner, J.R., Holland, G., Lewis, R.W., Vrijhof, H., Walker, A.P., 1999. Eye irritation: updated reference chemicals data bank. Toxicol In Vitro 13, 505–510.

Bolton, M., Hodkinson, A., Boda, S., Mould, A., Panagioti, M., Rhodes, S., Riste, L., van Marwijk, H., 2019. Serious adverse events reported in placebo randomised controlled trials of oral naltrexone: a systematic review and meta-analysis. BMC medicine 17, 10.

Borgheti-Cardoso, L.N., Depieri, L.V., Kooijmans, S.A., Diniz, H., Calzzani, R.A., Vicentini, F.T., van der Meel, R., Fantini, M.C., Iyomasa, M.M., Schiffelers, R.M., Bentley, M.V., 2015. An in situ gelling liquid crystalline system based on monoglycerides and polyethylenimine for local delivery of siRNAs. Eur J Pharm Sci 74, 103–117.

Borne, J., Nylander, T., Khan, A., 2003. Vesicle formation and other structures in aqueous dispersions of monoolein and sodium oleate. J Colloid Interface Sci 257, 310–320.

Boudreau, D.M., Lapham, G., Johnson, E.A., Bobb, J.F., Matthews, A.G., McCormack, J., Liu, D., Campbell, C.I., Rossom, R.C., Binswanger, I.A., Yarborough, B.J., Arnsten, J.H., Cunningham, C.O., Glass, J.E., Murphy, M.T., Zare, M., Hechter, R.C., Ahmedani, B., Braciszewski, J.M., Horigian, V.E., Szapocznik, J., Samet, J.H., Saxon, A.J., Schwartz, R.P., Bradley, K.A., 2020. Documented opioid use disorder and its treatment in primary care patients across six U.S. health systems. J Subst Abuse Treat 112S, 41–48.

Boyd, B.J., Whittaker, D.V., Khoo, S.M., Davey, G., 2006. Lyotropic liquid crystalline phases formed from glycerate surfactants as sustained release drug delivery systems. Int J Pharm 309, 218–226.

Brunen, S., Bekier, N.K., Hiemke, C., Korf, F., Wiedemann, K., Jahn, H., Kiefer, F., 2019. Therapeutic drug monitoring of naltrexone and 6beta-naltrexol during anti-craving treatment in alcohol dependence: reference ranges. Alcohol alcohol 54, 51–55.

Caboi, F., Amico, G.S., Pitzalis, P., Monduzzi, M., Nylander, T., Larsson, K., 2001. Addition of hydrophilic and lipophilic compounds of biological relevance to the monoolein/water system. I. Phase behavior. Chem Phys Lipids 109, 47–62.

Carvalho, A.F., Heilig, M., Perez, A., Probst, C., Rehm, J., 2019a. Alcohol use disorders. Lancet 394, 781–792.

Carvalho, F.C., Sarmento, V.H., Chiavacci, L.A., Barbi, M.S., Gremiao, M.P., 2010. Development and in vitro evaluation of surfactant systems for controlled release of zidovudine. J Pharm Sci 99, 2367–2374.

Carvalho, V.F., de Lemos, D.P., Vieira, C.S., Migotto, A., Lopes, L.B., 2017a. Potential of Non-aqueous Microemulsions to Improve the Delivery of Lipophilic Drugs to the Skin. AAPS PharmSciTech 18, 1739–1749.

Carvalho, V.F.M., Migotto, A., Giacone, D.V., de Lemos, D.P., Zanoni, T.B., Maria-Engler, S.S., Costa-Lotufo, L.V., Lopes, L.B., 2017b. Co-encapsulation of paclitaxel and C6 ceramide in tributyrin-containing nanocarriers improve co-localization in the skin and potentiate cytotoxic effects in 2D and 3D models. Eur J Pharm Sci 109, 131–143.

Carvalho, V.F.M., Salata, G.C., de Matos, J.K.R., Costa-Fernandez, S., Chorilli, M., Steiner, A.A., de Araujo, G.L.B., Silveira, E.R., Costa-Lotufo, L.V., Lopes, L.B., 2019b. Optimization of composition and obtainment parameters of biocompatible nanoemulsions intended for intraductal administration of piplartine (piperlongumine) and mammary tissue targeting. Int J Pharm 567, 118460.

Chandrasekaran, S.K., Paul, D.R., 1982. Dissolution-controlled transport from dispersed matrixes. J Pharm Sci 71, 1399–1402.

Chang, C.M., Bodmeier, R., 1997. Swelling of and drug release from monoglyceride-based drug delivery systems. J Pharm Sci 86, 747–752.

Chen, S., John, J.V., McCarthy, A., Xie, J., 2020. New forms of electrospun nanofiber materials for biomedical applications. B, Journal mat chem in press.

Collet, J.H., Moreton, R.C., 2007. Modified release peroral dosage forms. In: Aulton, M.E. (Ed.), Aulton's Pharmaceutics. The Design and Manufacture of Medicines, Churchil Livingstone Elsevier, pp. 483–499.

Courtenay, A.J., McAlister, E., McCrudden, M.T.C., Vora, L., Steiner, L., Levin, G., Levy-Nissenbaum, E., Shterman, N., Kearney, M.C., McCarthy, H.O., Donnelly, R.F., 2020. Hydrogel-forming microneedle arrays as a therapeutic option for transdermal esketamine delivery. J Control Release 322, 177–186.

Cunningham, C.L., Gremel, C.M., Groblewski, P.A., 2006. Drug-induced conditioned place preference and aversion in mice. Nat Protoc 1, 1662–1670.

Davanco, M.G., Campos, D.R., Carvalho, P.O., 2020. In vitro - In vivo correlation in the development of oral drug formulation: a screenshot of the last two decades. Int J Pharm 580, 119210.

de Silva, J.P., Poulos, A.S., Pansu, B., Davidson, P., Kasmi, B., Petermann, D., Asnacios, S., Meneau, F., Imperor, M., 2011. Rheological behaviour of polyoxometalate-doped lyotropic lamellar phases. Eur Phys J E Soft Matter 34, 1–9.

Depieri, L.V., Borgheti-Cardoso, L.N., Campos, P.M., Otaguiri, K.K., Vicentini, F.T., Lopes, L.B., Fonseca, M.J., Bentley, M.V., 2016. RNAi mediated IL-6 in vitro knockdown in psoriasis skin model with topical siRNA delivery system based on liquid crystalline phase. Eur J Pharm Biopharm 105, 50–58.

Drummond, C.J., Fong, C., 2000. Surfactant self-assembly objects as novel drug delivery vehicles. Curr Opinion Colloid Interface Sci 4, 449–456.

Faller, C., Bracher, M., Dami, N., Roguet, R., 2002. Predictive ability of reconstructed human epidermis equivalents for the assessment of skin irritation of cosmetics. Toxicol In Vitro 16, 557–572.

Fong, W.K., Hanley, T., Boyd, B.J., 2009. Stimuli responsive liquid crystals provide 'on-demand' drug delivery in vitro and in vivo. J Control Release 135, 218–226.

Friedmann, P.D., Mello, D., Lonergan, S., Bourgault, C., O'Toole, T.P., 2013. Aversion to injection limits acceptability of extended-release naltrexone among homeless, alcohol-dependent patients. Subst Abus 34, 94–96.

Ganem-Quintanar, A., Quintanar-Guerrero, D., Buri, P., 2000. Monoolein: a review of the pharmaceutical applications. Drug Dev Ind Pharm 26, 809–820.

Giannola, L.I., De Caro, V., Giandalia, G., Siragusa, M.G., Tripodo, C., Florena, A.M., Campisi, G., 2007. Release of naltrexone on buccal mucosa: permeation studies, histological aspects and matrix system design. Eur J Pharm Biopharm 67, 425–433.

Giordani, B., Abruzzo, A., Prata, C., Nicoletta, F.P., Dalena, F., Cerchiara, T., Luppi, B., Bigucci, F., 2020. Ondansetron buccal administration for paediatric use: a comparison between films and wafers. Int J Pharm 580, 119228.

Guo, L.K., Wang, Z.Y., Lu, G.Y., Wu, N., Dong, G.M., Ma, C.M., Zhang, R.L., Song, R., Li, J., 2019. Inhibition of naltrexone on relapse in methamphetamine self-administration and conditioned place preference in rats. Eur J Pharmacol 865, 172671.

Helledi, L.S., Schubert, L., 2001. Release kinetics of acyclovir from a suspension of acyclovir incorporated in a cubic phase delivery system. Drug Dev Ind Pharm 27, 1073–1081.

Holmberg, A., Piculell, L., Schurtenberger, P., Olsson, U., 2004. Oil-continuous microemulsions mixed with an amphiphilic graft copolymer or with the parent homopolymer: Polymer–droplet interactions as revealed by phase behavior and light scattering. Colloid Surface A 250, 325–336.

Hosmer, J., Reed, R., Bentley, M.V., Nornoo, A., Lopes, L.B., 2009. Microemulsions containing medium-chain glycerides as transdermal delivery systems for hydrophilic and hydrophobic drugs. AAPS PharmSciTech 10, 589–596.

Hosmer, J.M., Shin, S.H., Nornoo, A., Zheng, H., Lopes, L.B., 2011. Influence of internal structure and composition of liquid crystalline phases on topical delivery of paclitaxel. J Pharm Sci 100, 1444–1455.

Hosmer, J.M., Steiner, A.A., Lopes, L.B., 2013. Lamellar liquid crystalline phases for cutaneous delivery of Paclitaxel: impact of the monoglyceride. Pharm Res 30, 694–706.

Hulse, G.K., Stalenberg, V., McCallum, D., Smit, W., O'Neil, G., Morris, N., Tait, R.J., 2005. Histological changes over time around the site of sustained release naltrexone-poly(DL-lactide) implants in humans. J Control Release 108, 43–55.

Johnson, B.A., 2007. Naltrexone long-acting formulation in the treatment of alcohol dependence. Ther Clin Risk Manag 3, 741–749.

Junqueira Garcia, M.T., Pedralino Goncalves, T., Sao Felix Martins, E., Silva Martins, T., Carvalho de Abreu Fantini, M., Regazi Minarini, P.R., Costa Fernandez, S., Cassone Salata, G., Biagini Lopes, L., 2018. Improvement of cutaneous delivery of methylene blue by liquid crystals. Int J Pharm 548, 454-465.

Kurnatowska, I., Banasiak, M., Daniel, P., Wagrowska-Danilewicz, M., Nowicki, M., Two cases of severe de novo colitis in kidney transplant recipients after conversion to prolonged-release tacrolimus. Transpl Int 23, 553-558.

Kyobula, M., Adedeji, A., Alexander, M.R., Saleh, E., Wildman, R., Ashcroft, I., Gellert, P.R., Roberts, C.J., 2017. 3D inkjet printing of tablets exploiting bespoke complex geometries for controlled and tuneable drug release. J Control Release 261, 207–215.

Laia, C.A.T., López-Cornejo, P., Costa, S.M.B., d'Oliveira, J., Martinho, J.M.G., 1998. Dynamic light scattering study of aot microemulsions with nonaqueous polar additives in an oil continuous phase. Langmuir 14, 3531–3537.
Lara, M.G., Bentley, M.V., Collett, J.H., 2005. In vitro drug release mechanism and drug loading studies of cubic phase gels. Int J Pharm 293, 241–250.
Li, H., Hardy, R.J., Gu, X., 2008. Effect of drug solubility on polymer hydration and drug dissolution from polyethylene oxide (PEO) matrix tablets. AAPS PharmSciTech 9, 437–443.
Liu, W.M., Scott, K.A., Dennis, J.L., Kaminska, E., Levett, A.J., Dalgleish, A.G., 2016. Naltrexone at low doses upregulates a unique gene expression not seen with normal doses: Implications for its use in cancer therapy. Int J Oncol 49, 793–802.
Lobmaier, P., Gossop, M., Waal, H., Bramness, J., 2010. The pharmacological treatment of opioid addiction–a clinical perspective. Eur J Clin Pharmacol 66, 537–545.
Lopes, L.B., Lopes, J.L., Oliveira, D.C., Thomazini, J.A., Garcia, M.T., Fantini, M.C., Collett, J.H., Bentley, M.V., 2006. Liquid crystalline phases of monoolein and water for topical delivery of cyclosporin A: characterization and study of in vitro and in vivo delivery. Eur J Pharm Biopharm 63, 146–155.
Loureiro, A., Nogueira, E., Azoia, N.G., Sarria, M.P., Abreu, A.S., Shimanovich, U., Rollett, A., Harmark, J., Hebert, H., Guebitz, G., Bernardes, G.J., Preto, A., Gomes, A.C., Cavaco-Paulo, A., 2015. Size controlled protein nanoemulsions for active targeting of folate receptor positive cells. Colloids Surf B Biointerfaces 135, 90–98.
Mahdi, E.S., Noor, A.M., Sakeena, M.H., Abdullah, G.Z., Abdulkarim, M.F., Sattar, M.A., 2011. Formulation and in vitro release evaluation of newly synthesized palm kernel oil esters-based nanoemulsion delivery system for 30% ethanolic dried extract derived from local Phyllanthus urinaria for skin antiaging. Int J Nanomedicine 6, 2499–2512.
Makai, M., Csanyi, E., Nemeth, Z., Palinkas, J., Eros, I., 2003. Structure and drug release of lamellar liquid crystals containing glycerol. Int J Pharm 256, 95–107.
Malonne, H., Fontaine, J., Moës, A., 2000. In vitro/in vivo characterization of a tramadol HCl depot system composed of monoolein and water. Biol Pharm Bull 23, 627–631.
Manthey, J., Shield, K.D., Rylett, M., Hasan, O.S.M., Probst, C., Rehm, J., 2019. Global alcohol exposure between 1990 and 2017 and forecasts until 2030: a modelling study. Lancet 393, 2493–2502.
McMasters, J., Poh, S., Lin, J.B., Panitch, A., 2017. Delivery of anti-inflammatory peptides from hollow PEGylated poly(NIPAM) nanoparticles reduces inflammation in an ex vivo osteoarthritis model. J Control Release 258, 161–170.
Migotto, A., Carvalho, V.F.M., Salata, G.C., da Silva, F.W.M., Yan, C.Y.I., Ishida, K., Costa-Lotufo, L.V., Steiner, A.A., Lopes, L.B., 2018. Multifunctional nanoemulsions for intraductal delivery as a new platform for local treatment of breast cancer. Drug Deliv 25, 654–667.
Milewski, M., Stinchcomb, A.L., 2011. Vehicle composition influence on the microneedle-enhanced transdermal flux of naltrexone hydrochloride. Pharm Res 28, 124–134.
Mitchell, J.M., Bergren, L.J., Chen, K.S., Rowbotham, M.C., Fields, H.L., 2009. Naltrexone aversion and treatment efficacy are greatest in humans and rats that actively consume high levels of alcohol. Neurobiol disease 33, 72–80.
Mojeiko, G., de Brito, M., Salata, G.C., Lopes, L.B., 2019. Combination of microneedles and microemulsions to increase celecoxib topical delivery for potential application in chemoprevention of breast cancer. Int J Pharm 560, 365–376.
Muller-Goymann, C.C., 2004. Physicochemical characterization of colloidal drug delivery systems such as reverse micelles, vesicles, liquid crystals and nanoparticles for topical administration. Eur J Pharm Biopharm 58, 343–356.
Ng, W.Y., Migotto, A., Ferreira, T.S., Lopes, L.B., 2017. Monoolein-alginate beads as a platform to promote adenosine cutaneous localization and wound healing. Int. J. Biol. Macromol. 102, 1104–1111.
Ngo, H.T., Arnold-Reed, D.E., Hansson, R.C., Tait, R.J., Hulse, G.K., 2008. Blood naltrexone levels over time following naltrexone implant. Prog Neuropsychopharmacol Biol Psych. 32, 23–28.
Norling, T., Lading, P., Engstrom, S., Larsson, K., Krog, N., Nissen, S.S., 1992. Formulation of a drug delivery system based on a mixture of monoglycerides and triglycerides for use in the treatment of periodontal disease. J Clin Periodontol 19, 687–692.
Parker, L.A., Rennie, M., 1992. Naltrexone-induced aversions: assessment by place conditioning, taste reactivity, and taste avoidance paradigms. Pharmacology, Biochem. Behav. 41, 559–565.
Patel, V., Chisholm, D., Parikh, R., Charlson, F.J., Degenhardt, L., Dua, T., Ferrari, A.J., Hyman, S., Laxminarayan, R., Levin, C., Lund, C., Medina Mora, M.E., Petersen, I., Scott, J., Shidhaye, R., Vijayakumar, L., Thornicroft, G., Whiteford, H., 2016. Addressing the burden of mental, neurological, and substance use disorders: key messages from Disease Control Priorities, 3rd edition. Lancet 387, 1672-1685.
Pepe, D., McCall, M., Zheng, H., Lopes, L.B., 2013. Protein transduction domain-containing microemulsions as cutaneous delivery systems for an anticancer agent. J Pharm Sci 102, 1476–1487.
Phelps, J., Bentley, M.V., Lopes, L.B., 2011. In situ gelling hexagonal phases for sustained release of an anti-addiction drug. Colloids Surf B Biointerfaces 87, 391–398.
Rizwan, S.B., Hanley, T., Boyd, B.J., Rades, T., Hook, S., 2009. Liquid crystalline systems of phytantriol and glyceryl monooleate containing a hydrophilic protein: Characterisation, swelling and release kinetics. J Pharm Sci 98, 4191–4204.
Roozen, H.G., de Waart, R., van den Brink, W., 2007. Efficacy and tolerability of naltrexone in the treatment of alcohol dependence: oral versus injectable delivery. Eur Addict Res 13, 201–206.
Ruel-Gariepy, E., Leroux, J.C., 2004. In situ-forming hydrogels–review of temperature-sensitive systems. Eur J Pharm Biopharm 58, 409–426.
Sakaeda, T., Kobuchi, S., Yoshioka, R., Haruna, M., Takahata, N., Ito, Y., Sugano, A., Fukuzawa, K., Hayase, T., Hayakawa, T., Nakayama, H., Takaoka, Y., Tohkin, M., 2018. Susceptibility to serious skin and subcutaneous tissue disorders and skin tissue distribution of sodium-dependent glucose co-transporter type 2 (SGLT2) inhibitors. Int. J. Med. Sci. 15, 937–943.
Schmitz, J.M., Lindsay, J.A., Green, C.E., Herin, D.V., Stotts, A.L., Moeller, F.G., 2009. High-dose naltrexone therapy for cocaine-alcohol dependence. Am J Addict 18, 356–362.
Semlin, L., Schafer-Korting, M., Borelli, C., Korting, H.C., 2011. In vitro models for human skin disease. Drug Discov Today 16, 132–139.
Sikora, M., Rakowska, A., Olszewska, M., Rudnicka, L., 2019. The use of naltrexone in dermatology. current evidence and future directions. Current drug targets 20, 1058–1067.
Stevenson, C.L., Bennett, D.B., Lechuga-Ballesteros, D., 2005. Pharmaceutical liquid crystals: the relevance of partially ordered systems. J Pharm Sci 94, 1861–1880.
Sushchyk, S., Xi, Z.X., Wang, J.B., 2016. Combination of levo-tetrahydropalmatine and low dose naltrexone: a promising treatment for prevention of cocaine relapse. J Pharmacol Exp Ther 357, 248–257.
Verebey, K., Volavka, J., Mule, S.J., Resnick, R.B., 1976. Naltrexone: disposition, metabolism, and effects after acute and chronic dosing. Clinical Pharmacol Ther 20, 315–328.
Verhulst, C., Coiffard, C., Coiffard, L.J., Rivalland, P., De Roeck-Holtzhauer, Y., 1998. In vitro correlation between two colorimetric assays and the pyruvic acid consumption by fibroblasts cultured to determine the sodium laurylsulfate cytotoxicity. J Pharmacol Toxicol Methods 39, 143–146.
Victorri-Vigneau, C., Spiers, A., Caillet, P., Bruneau, M., Ignace, C., Challet-Bouju, G., Grall-Bronnec, M., 2018. Opioid antagonists for pharmacological treatment of gambling disorder: are they relevant? Curr neuropharmacol 16, 1418–1432.
Wang, Z., Diao, Z., Liu, F., Li, G., Zhang, G., 2006. Microstructure and rheological properties of liquid crystallines formed in Brij 97/water/IPM system. J Colloid Interface Sci 297, 813–818.
White, D.A., Hwang, M.L., Holtzman, S.G., 2005. Naltrexone-induced conditioned place aversion following a single dose of morphine in the rat. Pharmacol Biochem Behavior 81, 451–458.
Williams, K.L., Broadbridge, C.L., 2009. Potency of naltrexone to reduce ethanol self-administration in rats is greater for subcutaneous versus intraperitoneal injection. Alcohol 43, 119–126.
Yadav, S.K., Mishra, S., Mishra, B., 2012. Eudragit-based nanosuspension of poorly water-soluble drug: formulation and in vitro-in vivo evaluation. AAPS PharmSciTech 13, 1031–1044.
Yang, Y., Zhu, T., Liu, Z., Luo, M., Yu, D.G., Annie Bligh, S.W., 2019. The key role of straight fluid jet in predicting the drug dissolution from electrospun nanofibers. Int J Pharm 569, 118634.
Yin, W., Akala, E.O., Taylor, R.E., 2002. Design of naltrexone-loaded hydrolyzable crosslinked nanoparticles. Int J Pharm 244, 9–19.